UNIVERSITY OF TWENTE.

MASTER THESIS

Aerial Images Sea Lion Counting With Deep Learning: A Density Map Approach

Student:
Chirag Prabhakar Padubidri
S1995324

Committee University of Twente:
Prof. Dr. P.J.M. Havinga
DR. A. Kamilaris
Ir. E. Molenkamp

Faculty of Electrical Engineering, Mathematics & Computer Science
Pervasive Systems

Acknowledgment

This research is the product of collective effort put in by many people and I would take this opportunity to acknowledge their contributions. First and foremost, I would like to thank my daily supervisor Dr. Andreas Kamilaris for all his valuable guidance, for the time he has invested in me which has enhanced my critical thinking ability and all the encouragement that pushed me forward to delivery my best.

I would also like to extend my deepest gratitude to my committee Prof. Dr. Paul Havinga and Ir. E. Molenkamp for their precious time and helping me to quickly finish my graduation process. Furthermore, I am very much indebted to Dr. Savvas Karatsiolis (RISE, Cyprus) for his technical inputs throughout my thesis. I would also like to remember and thank Dr. Nirvana Meratnia for organizing my thesis work in pervasive systems group. I would like to give thanks to Jacob Kamminga for his inputs and Pervasive System group members for making my stay during the thesis work a comfortable one.

Finally, I would like to acknowledge and thank Ms. Nicole Baveld for her support and quick replies. Last but not least, I would like to express my hearty gratitude to my parents, family, and all my friends for their unwavering faith in me and undying support that kept me strong through the entire journey of my master program.

Abstract

The ability to automatically count animals may be essential for their survival. Out of all living mammals on Earth 60% are livestock, 36% humans, and only 4% are animals that live in the wild. In a relatively short period, human development of civilization caused a loss of 83% of all wildlife and 50% of all plants. The rate of species extinctions is accelerating. Wildlife surveys provide a population estimate and are conducted for various reasons such as species management, biology studies, and long term trend monitoring. In this thesis, we propose the use of deep learning (DL), together with satellite imagery, to count the numbers of sea lions with high precision. The proposed approach shows promising results than the state-of-art DL models used for counting, indicating that proposed method has the potential to be used more widely in large-scale wildlife surveying projects and initiatives.

Contents

List of Figures

Acronyms

ANN Artificial Neural Network.

CCNN Count Convolutional Neural Network.

CNN Convolutional Neural Network.

GPU Graphical Processing Unit.

MAE Mean Absolute Error.

NOAA National Oceanic and Atmospheric Administration.

PCA Principal Component Analysis.

R-CNN Region-Based Convolutional Neural Network.

ReLu Rectified Linear Unit.

RMSE Root Mean Square Error.

SVM Support Vector Machine.

Chapter 1

Introduction

The ability to automatically count animals may be essential for their survival. Out of all living mammals on Earth 60 % are livestock, 36 % humans, and only 4 % are animals that live in the wild [11]. In a relatively short period, human development of civilization caused a loss of 83 % of all wildlife and 50 % of all plants. Moreover, the current rate of the global decline in wildlife populations is unprecedented in human history – and the rate of species extinctions is accelerating [12], [13]. Wildlife surveys provide a population estimate and are conducted for various reasons such as species management, biology studies, and long term trend monitoring. This information may be essential for species survival. For example, biologists use population trends to investigate the effect of environmental factors such as human activity in a region on a species' population. This information can be used to change international policies to benefit wildlife conservation. Using satellites or airplanes allows biologists to survey remote species across vast areas. However, current counting methods are laborious, expensive, and limited. Automating the counting from photographs dramatically speeds up wildlife surveys and frees up human resources for other critical tasks. Moreover, automatic counting supports a higher frequency of surveys to get better insights into population trends.

NOAA Fisheries Alaska Fisheries Science Center conducts one such animal survey to count Steller sea lions'.The Steller (or northern) sea lion is the largest member of the family *Otariidae*, the "eared seals". In the 90's Steller sea lions used to be highly abundant throughout many parts of the coastal North Pacific Ocean. Indigenous peoples and settlers hunted them for their meat, fur, oil, and other products. In the western Aleutian Islands alone, this species declined 94% in the last 30 years. Because of this widespread population decline, Steller sea lions have been listed as endangered species under the Endangered Species Act (ESA) in 1990 [14]. The endangered western population of sea lions, found in the North Pacific, are the focus of conservation efforts that require annual population counts. Having accurate population estimates enables us to better understand factors that may be contributing to a lack of recovery of Steller sea lions in this area, despite the conservation efforts. Specially trained scientists at NOAA Fisheries Alaska Fisheries Science Center conducts this survey using airplanes and unmanned aircraft systems to collect aerial images [15]. Then trained biologists count the sea lions from the thousands of images collected which takes up to four months for this task. Once individual counts are conducted, the tallies are be reconciled to confirm their reliability. The results of these counts are time-sensitive.

Automating the manual counting process will free up critical resources allowing them to focus more on the actual conservation of sea lions. Therefore, to optimize the counting process, the NOAA Fisheries organized a Kaggle competition dating June 2017, seeking developers to build algorithms which accurately count the number of sea lions in aerial photographs [16].

1.1 Research Question

In this thesis, we use a novel deep learning (DL) algorithm to automatically count Sea Lions from Aerial Images. We use the dataset from a Kaggle competition [16] that invited participants to develop algorithms that accurately count the number of sea lions in aerial photographs. DL is a powerful technique that has demonstrated excellent performance for a wide range of application domains such as image processing and data analysis [17], [18]. DL extends machine learning (ML) by adding more "depth" (complexity) into the model, transforming the data using various functions that hierarchically allow data representation, through several abstraction levels. Compared to traditional techniques such as Support Vector Machines and Random Forests, DL has demonstrated enhanced performance in classification and counting computer vision-related problems [19].
This research work seeks to address the research question;

"How density map approach could be used for counting task using segmentation algorithm?"
While developing a DL algorithm for automatic sea lions' counting we also answer the following research sub-questions:

- What are the different available counting techniques?
- What are the best counting techniques and data annotation for densely crowded dataset?
- How do the proposed algorithm affected by a complex background environment in images?
- Where does the proposed algorithm stands with the Kaggle competition?

1.2 Thesis Outline

The thesis is organized as follows;

- Chapter 2, provides the background for Deep Learning in Computer Vision, where we discuss the Image Classification, Object detection and Localization, Segmentation, and related work for different counting techniques.
- In Chapter 3, we deal with dataset construction and preprocessing techniques.
- In Chapter 4, we discuss our implemented methodology.
- In Chapter 5, we evaluate the performance of the proposed algorithm.
- Finally, Chapter 6 concludes the thesis and presents a section for future work.

Chapter 2

Background/Related Works

2.1 Deep Learning Methods in Computer Vision

Image classification, object detection and localization are some of the major challenges in computer vision. DL methods such as Convolutional Neural Networks (CNN) have pushed the limits of traditional computer vision techniques to solve these challenges. Deep learning (DL) is a branch of machine learning that uses Artificial Neural Networks (ANN)[1] with many layers. A deep neural network analyzes data with learned representations similar to the way a person would look at a problem. Rapid progressions in DL and improvements in device capabilities including computing power, memory capacity, power consumption, image sensor resolution, and optics have improved the performance and cost-effectiveness of further quickened the spread of vision-based applications [20].

2.1.1 Image Classification

Image Classification is a systematic arrangement of images in groups and categories based on its features i.e. in simple words for a given input image, outputting the class labels or the probability that input image is of a particular class, as shown in Figure.2.1. Before DL, the traditional Computer Vision (CV) techniques used hand-crafted feature extraction for classification. Features are individual measurable or informative properties of an image. CV algorithms used edge detection, corner detection or threshold segmentation algorithms to extract features. Each individual class will have its own distinct features, based on which classification is done. The difficulty with the CV approach is that it requires choosing which features are important in each given image for each class. As the number of classes to classify

[1] ANN are computing systems vaguely inspired by the biological neural networks that constitute animal brains.

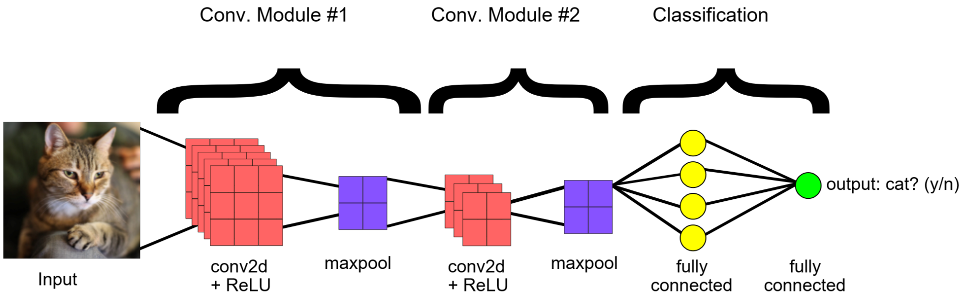

Figure 2.1: Simple CNN model representing image classification [1]

increases, feature extraction will become a more complex task.

The DL's Convolutional Neural Network (CNN) solves this problem, it uses convolutional layers for feature extraction eliminating the manual feature extraction. A typical CNN classifier architecture consist of repeated blocks of Convolutional layer with activation function followed by max-pooling layer and finally a fully connected layer with output Neurons matching number of class as shown in Figure.2.1.

- **Convolutional layers** are nothing but a set of learn-able 2D filters. Each filter learns how to extract features and patterns present in the image. The filter is convolved across the width and height of the input image, and a dot product operation is computed to give an activation map.

- After each convolution operation, an **Activation function** is added to decide whether that particular neuron fires or not. The activation function is a mathematical equation that determines the output of a neuron. There are different activation functions with different characteristics as illustrated in Figure.2.2.

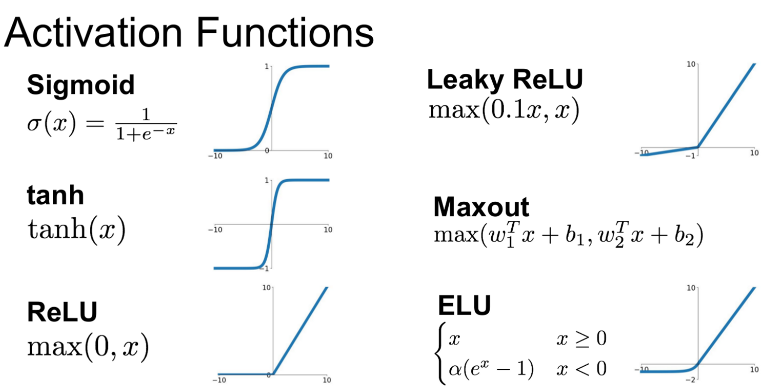

Figure 2.2: Few commonly used activation functions [2]

- Different filters that detect different features are convolved with the input image and the activation maps are stacked together to form the input for the next layer. By stacking more activation maps, we can get more abstract features. However, as the architecture becomes deeper, we may consume too much memory. In order to solve this problem, **Pooling layers** are used to reduce the dimension of the activation maps. Pooling layers will discard a few values either by keeping maximum value (Max Pooling) or by averaging the values (Average Pooling). By discarding some values in each filter, the dimension of the activation map is reduced. This means that if some features have already been identified in the previous convolution operation, then a detailed image is no longer needed for further processing, and it is compressed to less detailed pictures.

- Finally, the convolution blocks is connected to **Fully Connected layer** which takes the output information from convolutional networks converting into an N-dimensional vector, where N is the number of classes, and each N value representing the probability of being a certain class.

AlexNet, VGG, ResNet etc are few state-of-art classification architectures. These will have 100's of feature extraction hidden layer. Once such example architecture, AlexNet is shown in Figure.2.3

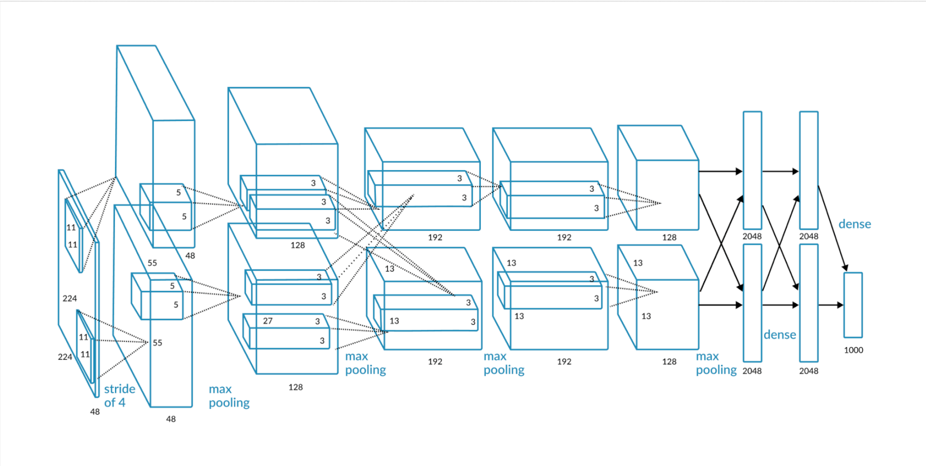

Figure 2.3: Alenet block diagram [3]

2.1.2 Object Detection and Localization

Object detection and Localization is an automated method for locating interesting object or multiple objects in an image with respect to the background i.e. given an input image possibly with multiple objects, we need to generate a bounding box around each object and classify the objects, as shown in Figure.2.4.

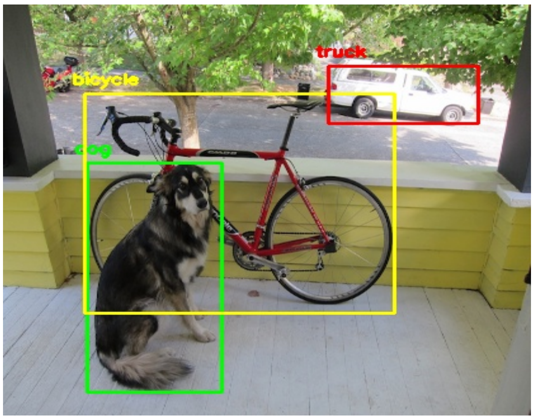

Figure 2.4: Object detection and localization with bounding box [4]

The general idea behind object detection and Localization is to predict the probability of the object being in a class (label) along with the coordinates of the object location. Predicting label is a classification problem and generating coordinates can be seen as regression problem[2], which is illustrated in Figure.2.5. The total loss for the architecture will be a combination of classification loss and regression loss.

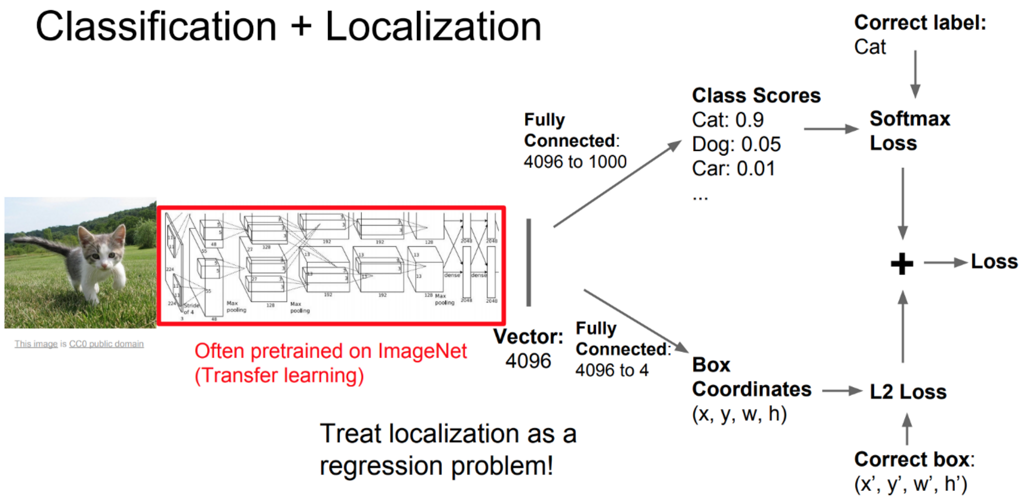

Figure 2.5: NN architecture representation for object detection and localization [5]

Multiple object detection and localization tasks can be solved with two approaches, which lead to two different categories of object detection algorithm.

- **Two-Stage Method:** This method will first perform a region proposal. This means regions highly likely to contain an object are selected either with traditional computer vision techniques (like selective search), or by using a deep learning-based region proposal network (RPN). Once a small set of candidate

[2]Regression is a statistical approach to find the relationship between variables

windows is gathered, we can formulate a set of number of regression models and classification models to solve the object detection problem. This category includes algorithms like Faster R-CNN [21], R_FCN [22], and FPN-FRCN [23]. Algorithms in this category are usually called two-stage methods. They are generally more accurate, but slower than the single-stage method which is discussed below.

- **Single-Stage Method:** This method only looks for objects at fixed locations with fixed sizes. These locations and sizes are strategically selected so that most scenarios are covered. These algorithms usually separate the original images into fixed-size grid regions. For each region, these algorithms try to predict a fixed number of objects of certain, pre-determined shapes and sizes. Algorithms belonging to this category are called single-stage methods. Examples of such methods include YOLO [24], SSD [25] and RetinaNet [26]. Algorithms in this category usually run faster but are less accurate. This type of algorithm is often utilized for applications requiring real-time detection.

Example

R-CNN was one of the state-of-art object detection architecture described in [6] (2014) by Ross Girshick, et al. from UC Berkeley. It was one of the first large and successful application of convolutional neural networks to the problem of object localization, detection, and segmentation. The approach had achieved then state-of-the-art results on the VOC-2012 dataset and the 200-class ILSVRC-2013 object detection dataset. The proposed R-CNN model is comprised of three modules;

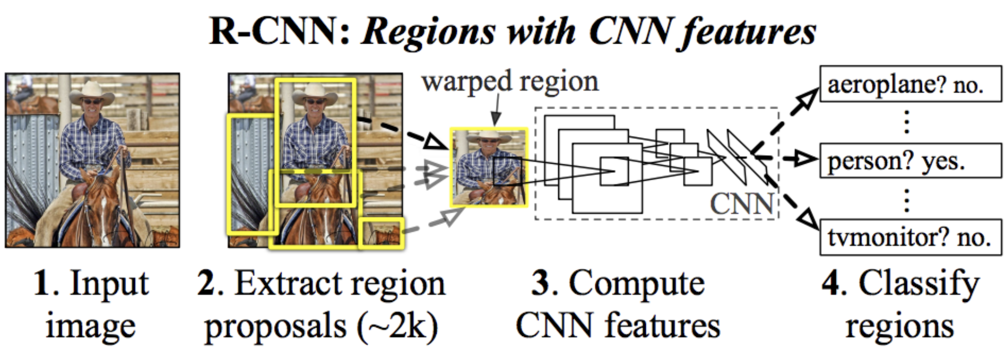

Figure 2.6: RCNN model architecture [6]

- **Module 1: Region Proposal.** Extracts independent ROI from the image. A computer vision technique is used to propose candidate regions or bounding boxes of potential objects in the image called “selective search,” although the flexibility of the design allows other region proposal algorithms to be used.

- **Module 2: Feature Extractor.** Extract features from each ROI. The feature extractor used by the model was the AlexNet. The output of the CNN was a 4,096 element vector that describes the contents of the image.

- **Module 3: Classifier.** Classifies features as one of the known classes. A linear SVM for classification is used, specifically one SVM is trained for each known class.

2.1.3 Image Segmentation

Semantic segmentation:

Semantic segmentation, or image segmentation, is the task of clustering parts of an image together that belong to the same object class. It is a form of pixel-level prediction i.e. image classification at the pixel level, because each pixel in an image is classified according to a category as shown in Figure.2.7.a. Since the problem is defined at the pixel level, determining only image class labels and location is not acceptable, but localizing them at the original image pixel resolution is necessary.

A general semantic segmentation architecture can be broadly thought of an **encoder** network followed by an **decoder** network.

- The **Encoder** is usually a pretrained classification architecture like AlexNet, VGG, or ResNet, which takes an input image and generates a high-dimensional feature vector.

- **Decoder**, semantically projects the discriminative features (lower resolution) learned by the encoder onto the pixel space (higher resolution) to get a dense classification.

Semantic segmentation not only requires discrimination at pixel level but also a mechanism to project the discriminative features learn at different stages of the encoder onto the pixel space.

Instance Segmentation:

Instance segmentation is a sub-type of image segmentation that identifies each instance of each object within the image at the pixel level, shown in Figure.2.7.b. Instance segmentation is an important step to achieving a comprehensive image recognition and object detection algorithms.

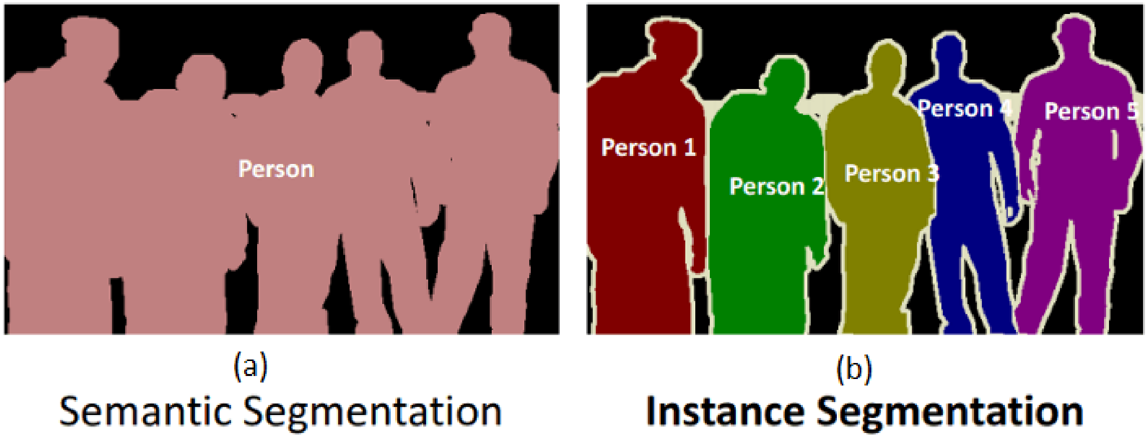

Figure 2.7: Sample for semantic segmentation [7]

2.1.4 Image Annotation:

Image annotation is the first task in Deep learning. Image annotation is the human-powered task of annotating an image with labels. It helps the algorithm to learn certain patterns and store that into virtual memory to correlate or utilize the same while analyzing similar data comes into real-life use. Bounding box, Polygon Annotation, 3D Cuboid, Semantic Segmentation, Landmarking, Dot Annotation are few types of image annotation used for different applications as illustrated in Figure.2.8. These annotated images are used for training the model.

2.1.5 Counting Related Works

Counting objects is a challenging task for computer vision algorithms, especially when the instance of objects varies in shape, color, or size. The state-of-art algorithms has demonstrated that DL can obtain good counting performance on these images. One of the easiest ways of counting objects using DL is first detecting the object using CNN, and then count all found instances. This is effective but requires bounding box annotation which is time-consuming especially when objects are heavily crowded. The simplest annotation for highly crowded images is dot-annotation, here a dot is marked on the center of each object which is used for training DL model. So based on the annotation methods used to label the dataset, we have divided the related works for deep-learning based counting algorithms into 3 categories;

Count via detection

In this method, a visual object detector is used to localize individual object instances in the image. Given the localization, counting becomes trivial. In this case, objects

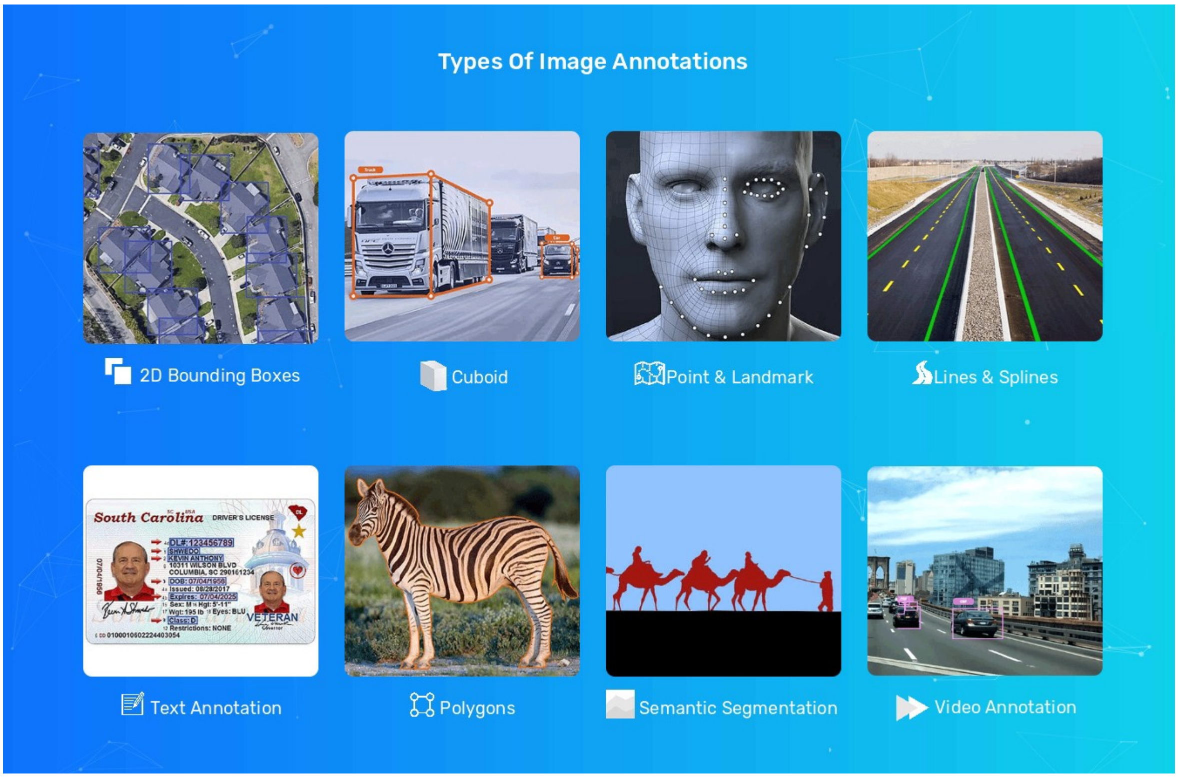

Figure 2.8: Different types of annotations used in Deep learning for image annotation [8]

are annotated by a bounding box. Several methods [27], [28], [29], use this type of detection for counting objects. For instance in [27], the authors use the NOAA sea lion dataset proposing a sliding window detection and classification algorithm for counting sea lions. However, counting via detection suffer from occlusion among objects. Moreover, the annotation of densely crowed images is expensive.

Count via image-level regression

This way of counting is based on image-level label regression which is the least expensive annotation technique. In [30], the authors proposed a regression model for counting tomatoes, where the model learns directly from the input image and predicts the number of tomatoes in the image. Authors claim an accuracy of 91% on real images. Furthermore, the winner of the Kaggle Sealion competition [31] used an image regression method for count estimation. The methods mentioned above can only perform counting but not localization of the object. Thus, they cannot be used in cases where we are interested in both counting as well as localization of the objects.

Count via density map

In this case, annotation involves marking a point corresponding to each object's location in the image from which a density heat map is generated, wchi is used for training. The density map gives the spatial distribution of objects in a given image relative to the total number of objects, which helps us better understand the scene information and reduce the effect of occlusion. The Learning-to-count model of [32] introduces a counting approach, which works by learning a linear mapping from local image features to object density maps. By properly training the DL model, one can estimate the object count by simply integrating over regions in the density map produced by the model. The same strategy has also been followed in [33], [34] and [35]. The novel model called Counting CNN (CCNN) and Hydra CNN were proposed in [34] for counting crowd density. Essentially, the CCNN model is formulated as a regression model where the network learns how to map the appearance of the image patches to their corresponding object density maps. The Hydra CNN constitutes a scale-aware counting model in order to estimate object densities in various heavily-crowded scenarios where no geometric information of the scene can be provided. Similarly, the authors in [35] proposed a modified CCNN model, which is a model composed of a combination of CCNN and ResNeXt, to estimate the pig density in pig livestock farms. [33] proposed the DisCountNet model, a two-stage network that uses theories from both detection and density-map networks. At the first stage, DiscNet performs a coarse detection of the patches of images from a larger input image which has dense objects. Following this, the CountNet model operates on the dense regions of the sparse matrix to generate a density map, which provides fine locations and count predictions on densities of objects. Here, the author makes a few assumptions based on observations made on the dataset. Thus, this method needs prior information about the dataset while choosing the parameters.

Summing up, the counting techniques mentioned above, it revolve around two distinct characteristics of the input data:

1. Sparse data which favors detection networks.

2. Dense data where density map networks are used.

2.2 Summary

In this chapter we saw various types of deep learning architecture solving different problems. Figure.2.9 demonstrate the output of classification, Object detection, Semantic segmentation, and Object Instance Segmentation method on a given input image.

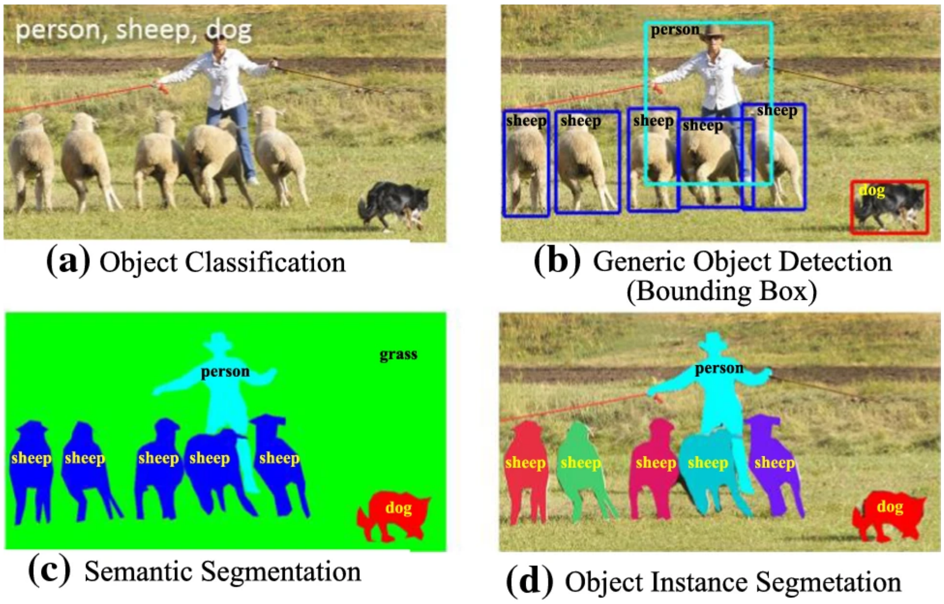

Figure 2.9: Output of different types of Deep learning application in Computer Vision [9]

In this thesis work, our solution treat sea lion counting problem as counting via density map. The proposed model uses semantic segmentation algorithms for density estimation without pixel-level annotation. We use dot annotation i.e. placing dots at the center of each animal and then generate a Gaussian density map from it, this largely reduces annotation overhead. The proposed solution greatly improves the counting and localization performance with minimum annotation.

Chapter 3

Dataset

3.1 Data Collection

The Steller Sea Lion dataset from NOAA fisheries [16], consists of 948 aerial images, which have different categories of sea lions based on age and gender of the animals: adult males (also known as bulls); sub-adult males; adult females; juveniles; and pups. For each image, there are two versions: the original image as well as the one with dots in the center of each sea lion. Image resolution was not uniform but was roughly around $5000X3000$, each image roughly occupying around 5MB. The dataset was split into training (0-800) and testing images (801-947) with 85:15 ratio respectively. The testing images were used for assessing the model's performance. During this phase, the following observations were made on the dataset:

1. The large image resolution gave better details (Figure.3.1.a), but required large memory size(RAM).

2. The number of sea lions per images varied widely between 3 and 900 animals

3. In most of the images, the sea lions were gathered together in the same place, leaving large portions of the image with only background

3.2 Data Preparation

To address the observations and challenges described in previous Section, we performed few image pre-processing methods which is illustrated in Figure.3.1.

- First, we used rough cropping to remove the portion of image which had only background, refer Figure.3.1b.

- We set the input image size to $256X256$. Instead of resizing the original image, we used sliding window cropping with roughly 10% overlap. Approximately, 180000 images of resolution $256X256$ was generated, refer Figure.3.1c
- Post cropping we noticed that few of the images did not had any Sea lions in it, an example is shown in Figure.3.1c crop 3 and 4. These images were discarded.

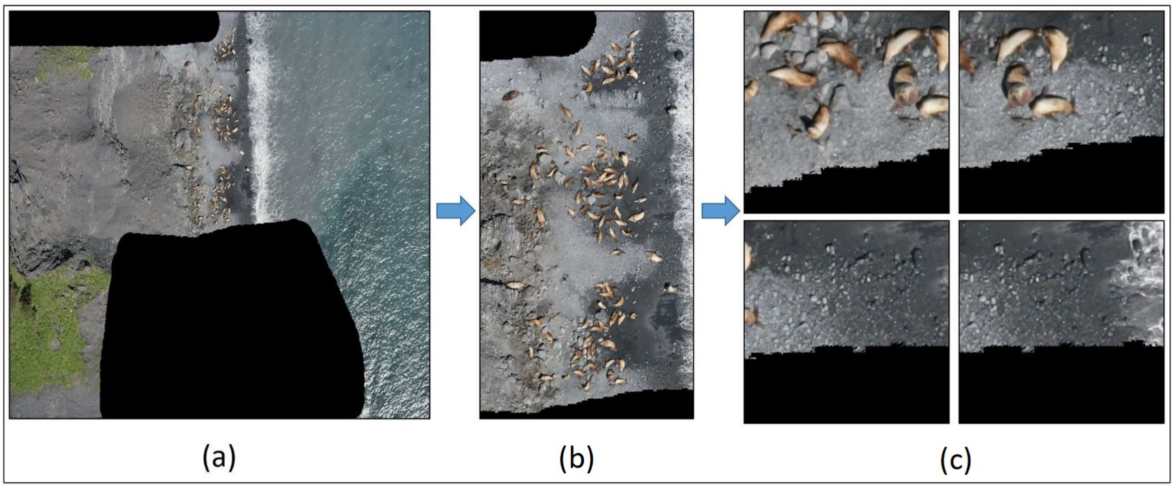

Figure 3.1: Data Preparation Workflow. **(a)** The original image with dimension 3328X4992. **(b)** Background removed image. **(c)** Sliding window cropped image of dimension 256X256

For the new training images with size $256X256$, the number of sea lion per image ranged from 1-80 with mean 4 and standard deviation 6. Table 3.1 shows the sea lions' distribution in the training dataset. Further, for training the train dataset was split into Train and Valid set with 80:20 ratio.

Table 3.1: Training images sea lions distribution per image

Sea lions per image	**Total no. of images**
01 - 20	54,870
21 - 40	1,468
>40	127

3.3 Summary

This chapter focused on Dataset used for our work. We discussed our observation on the dataset and propose the data preparation method. Post data preparation we were able to get 56465 Training images and 2842 testing image (Table 3.2).

Table 3.2: Training (Train+Valid) and Testing dataset split

Dataset	**No.of Images**
Training Images (Train+Val)	56465
Testing Images	2842

Chapter 4

Methodology

4.1 Overview

As discussed earlier, to estimate the number of objects in an image, there are generally three methods. One is to input the image, use an object detection algorithm to detect the object instances, and then count instance. Second, is to input the image, regress the input image and output the total count. And the last one is to input the image, predict the distribution density map, and get the number of object by summing the density distribution. Our solution treats the counting problem as the third one, an object density estimation task. The reasons are as follows:

- In general, the count via detection and count via regression are not accurate enough, and struggles especially when the objects are at different perspectives, different postures, and highly occluded.

- For example, count via regression directly gives the object count without having any distribution detail or scene information which makes it difficult to visualize the result. In count via detection a large number of candidate windows need to be detected during the detection process, which reduces the efficiency of the algorithm and is not suitable for scenes with multi-perspective and multi-object overlapping.

- The proposed density map approach gives the spatial distribution of objects in a given image relative to the total number of objects, which helps us to better understand the scene information. The object count can be counted by spatial integration, and local area analysis can be performed to produce more accurate numbers.

- Counting via density map is also more suitable for images with different perspective and occlusion.

Considering this an end-to-end model was designed that takes an input image and produces a density map with the precise localization of the animal. To generate density map a semantic segmentation model, UNet [36] is proposed.The main disadvantage of semantic segmentation algorithms is the tedious pixel-level annotation. Our solution uses dot annotation, which largely reduces annotation overhead. The proposed solution greatly improves the counting and localization performance with minimum annotation.

An illustration of the proposed solution is shown in Fig.4.1. The input image is fed to the proposed architecture, the Encoder section of the architecture generates a high dimensional feature vector. Decoder, semantically projects the feature learned by the encoder onto the pixel space generating corresponding density distribution for the given image. This density map is used to get the number of objects by simply integrating the density distribution over the region.

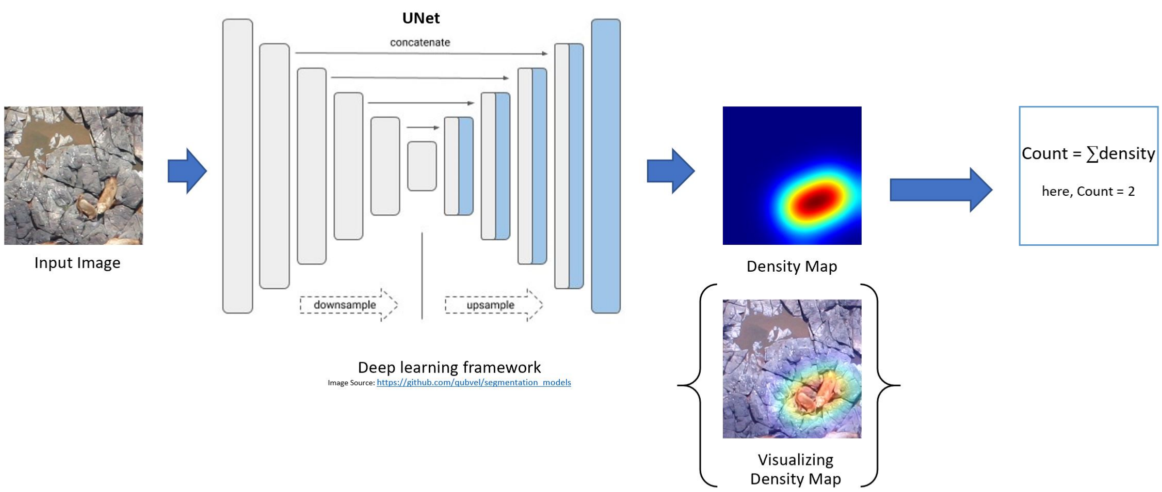

Figure 4.1: The proposed architecture block diagram

4.2 Density Map

In order to estimate the object count in an image, the model needs to learn from the density distribution of the individual image, and once the model learns to generate density distribution we need to calculate the total count from it. In this section we will formalize mathematical definition to generate a ground-truth density map and how we can arrive at the object count from predicted density map.

Table 4.1: Average size of Sea-lion based on their classes

Class	**Size(Avg)**
adult males	80X60
sub-adult males	70X40
adult females	60X40
juveniles	40X30
pups	30X20

4.2.1 Density Map Generation:

The Kaggle dataset consisted of sea lion images along with its corresponding dot annotated images. This dot annotation was done by expert NOAA biologists. The dotted images were used to extract the coordinates of the center of each sea lions which is used to generate the ground-truth density map. The density map is generated by processing the center of point objects with a Gaussian smoothing kernel, Figure.4.2.

For the given set of annotated images, where all the animals have been marked with dots, the ground truth density map D_I, for an image I, is defined as a sum of Gaussian functions centered at each dot annotation.

$$D_I(p) = \sum_{\mu \in A_I} \mathcal{N}(p; \mu, \Sigma), \tag{4.1}$$

where A_I is the set of 2D points annotation for image I and $\mathcal{N}(p;\mu,\Sigma)$ represents an isotropic 2D Gaussian function, with a mean μ and a covariance matrix Σ, evaluated at pixel position p. Covariance Σ=$\sigma^2 I$ is a diagonal matrix with σ controlling the spread of the distribution. Based on the average size of the sea lion, we chose $\sigma = 5$.

When 2 points intersects the density map of this intersection area is superimposed. Hence, the density map approach is suitable for problems with sparsely distributed objects as well as images with occlusion, overlapping, and varied perspectives.

Figure 4.2: Training image and corresponding ground-truth Gaussian density map

4.2.2 Counting from Density Map

The density map provides the spatial distribution of objects in a given image, relative to the total number of objects. Given the density map, D_I the total count N_I can be obtained by integrating the pixel values in density map D_I over the entire image as below:

$$N_I = \sum_{p \in I} D_I(p) \tag{4.2}$$

4.3 Model

The feed-forward regression networks in [34], [35] compress and encode images into smaller representation vectors. The combination of CCNN+ResNeXt model in [35] takes an input image of size $72X72$ and produces an output density map of size $18X18$. Due to down-sampling and the loss of spatial resolution in higher layers, there is a possibility to lose information. To avoid this, an encoder-decoder architecture, named *UNet* is proposed as a learning architecture.

UNet is a Convolutional Neural Network (CNN) architecture, proposed in [36] for biomedical image segmentation. UNet is an encoder-decoder-type network architecture for image segmentation. The name of the architecture comes from its distinct shape, where the feature maps from the down-sampling block are fed into the up-sampling block. The down-sampling path captures context and a symmetric up-sampling path enables precise localization.

Figure 4.3 shows the architecture of the UNet, where each gray box corresponds to a multi-channel feature map. Yellow box represents the downsampling block and the Blue box represents the Up-sampling block. The size and number of channels

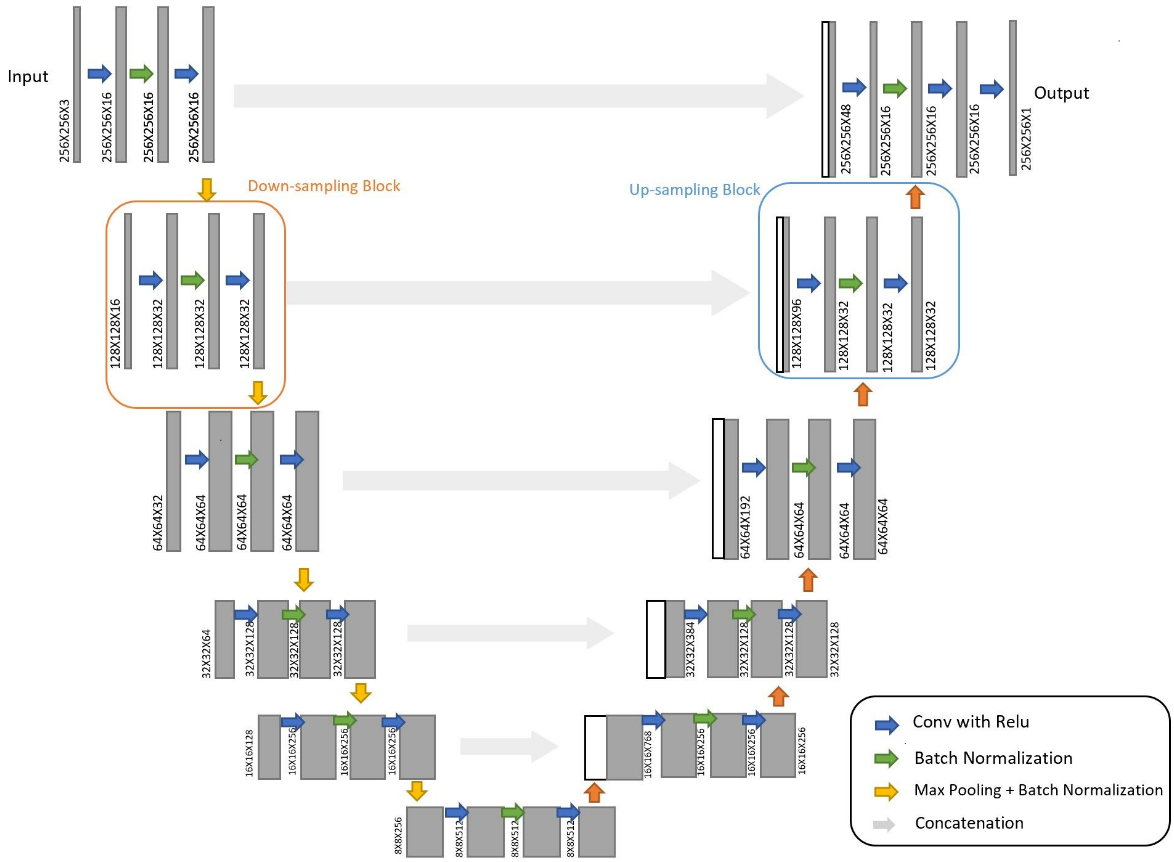

Figure 4.3: UNet Architecture

[x,y,c] is provided at the lower-left edge of the box. White boxes represent copied feature maps. The arrows denote the different operations.

The Down-sampling/Contracting path consists of the repeated application of two $3X3$ convolutions, each followed by a ReLU, batch-normalization layer, and a $2X2$ max pooling operation with stride 1. The number of feature channels (filter size) is doubled at each downsample block.

Similarly, the Up-sampling/Expansive path consists of a $2X2$ 2D up-sampling convolution with the nearest interpolation. The up-sampling of the feature maps halves the number of feature channels. This is concatenated with the correspondingly cropped feature map from the contracting path, which is followed with two $3X3$ convolutions, with ReLU activation. At the final layer, a $1X1$ convolution is used to map feature vector to the desired number of classes. The input data is normalized before feeding it into the network.

4.3.1 Implementation

To verify the effectiveness of the proposed network architecture, two models were trained:

Model-1

Model-1 is the basic UNet without any existing feature extractor architecture. The UNet architecture shown in figure 4.3 was implemented in Keras using a Tensorflow backend. The model have 5 downsampling block and 5 upsampling block. The figure 4.4 shows the total number of parameters for the implemented model.

```
==============================
Total params: 15,738,747
Trainable params: 15,732,763
Non-trainable params: 5,984
______________________________
```

Figure 4.4: Total number for parameters for Model-1 architecture

Model-2

Here an existing classification model with pre-trained weights is used as feature extraction. Resnet, Resnext, VGG19, Inceptionv3, densenet, inceptionresnetv2, mobilenet, efficientnetb are few state-of-art classification models that could be used as a feature extractor. Figure 4.5 show the comparison between different architectures. For our application we use Efficientnet version-'5' [10] as a feature extractor. Effiecientnet is a Convolutional Neural Network developed by google, that has set new records for both accuracy and computational efficiency. In high-accuracy regime, with 66M parameters and 37B FLOPS. At the same time, the model is 8.4x smaller and 6.1x faster on CPU inference than the former leader, Gpipe.

The architecture was implemented on Keras using TensorFlow backend [37]. EfficientNetB5 is used as a feature extractor to build the UNet model. All the layer was set as trainable. 'BatchNormalization' layer was used between the 2D-Convolution layer and activation. As we have only one class i.e. sea-lion class, the output activation was set to 'sigmoid' function instead of softmax. The model was initialized with 'Imagenet' pretrained weight. The figure 4.6 shows the summary of the model parameters.

4.3.2 Training Parameter

Loss Function:

To make model learn, an objective optimization function is defined, which measures the Root Mean Square Error(RMSE) between the predicted density map ($\hat{D}$) and the

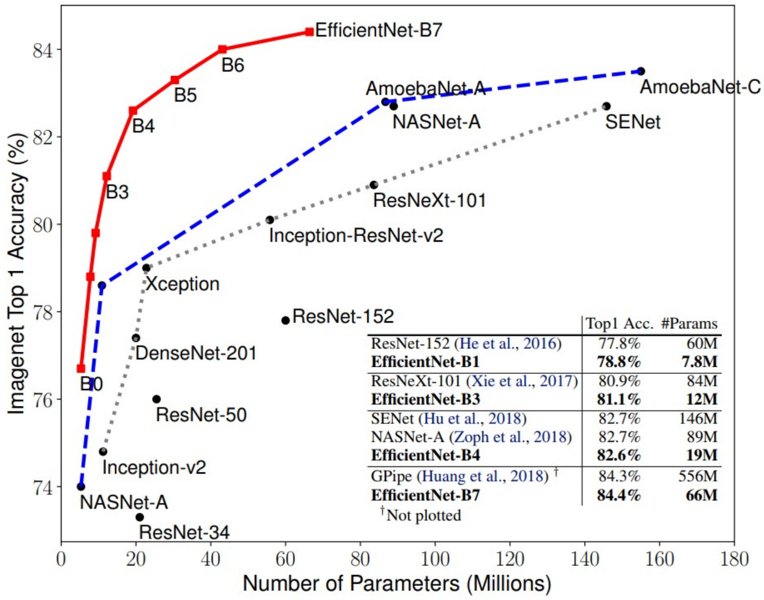

Figure 4.5: Comparison of different classification model [10]

```
================================
Total params: 37,468,673
Trainable params: 37,293,953
Non-trainable params: 174,720
________________________________
```

Figure 4.6: Total number for parameters for Model-2 architecture

true density map (D), defined as:

$$L = \sqrt{\frac{1}{N}\sum_{n=1}^{N}(\hat{D} - D)^2} \tag{4.3}$$

Optimizer:

All the parameters were optimized using Adam with a learning rate of 0.001. A learning rate reduction during training was also used for further improvement. The Nvidia GeForce RTX 2060 GPU was used for training, with a batch size of 8.

4.4 Summary

In this chapter we discussed the overview of the proposed architecture. We defined mathematical formulas for Gaussian based counting approach. The architecture description and their implementation details were mentioned. Finally the parameters used for the training the model was stated.

Chapter 5

Performance Evaluation

5.1 Training Results

Both models were trained for 100 epochs and their training results were logged. Basic UNet (*Model-1*) took 7 hours for training while UNet with the EfficientNet-B5 feature extractor (*Model-2*) took 17 hours. According to their performance on the validation dataset, early stopping was used for selecting the model with the best performance. Figure 5.1 shows the loss function gradient descent during training for Model-1 and Model-2. We can see that the Model-2 which used the 'Imagenet' pre-trained weights already having some prior information about the sea lions, converged faster than Model-1. Even though the plot shows that the loss converges to some small value for both models, the Model-2 was a little better in finding its minima.

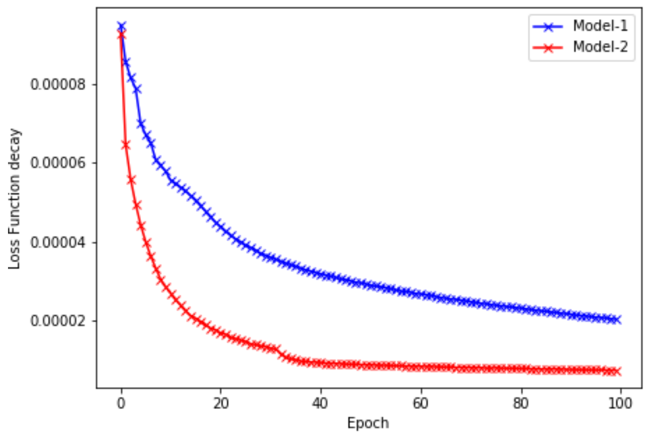

Figure 5.1: Training Loss function gradient vs. Iteration curve for Basic UNet (Model-1) and UNet with EfficientNet-B5 feature extractor architecture (Model-2)

5.2 Model Evaluation

5.2.1 Performance Metrics

For performance evaluation of the proposed models, we use Mean Absolute Error (MAE) and Root Mean Square Error (RMSE) to measure the accuracy of the predicted count.

Mean Absolute Error:

MAE is the average of the absolute differences between predicted and actual count. It measures the average magnitude of the errors in a set of predictions.

$$MAE = \frac{1}{N}\sum_{i=1}^{N} |(y_i - \hat{y}_i)| \tag{5.1}$$

where y_i is the actual sea lion count in the ith image, $\hat{y}_i$ is the predicted sea lion count in the ith image and N is the total number of test images.

Root Mean Square Error:

RMSE is the square root of the average of squared differences between predicted and actual count. Since the errors are squared before they are averaged, the RMSE gives a relatively high weight to large errors.

$$RMSE = \sqrt{\frac{1}{N}\sum_{i=1}^{N}(y_i - \hat{y}_i)^2}. \tag{5.2}$$

where y_i is the actual sea lion count in the ith image, $\hat{y}_i$ is the predicted sea lion count in the ith image and N is the total number of test images.

The MAE characterizes the accuracy of the algorithm, while the RMSE represents the degree of dispersion in the differences, and examines the robustness of the models.

5.2.2 Testing Results

The trained model was tested on the testing dataset and RMSE & MAE for animal count is recorded.

Table 5.1: Comparison table for Model-1 and Model-2

Model	RMS(Train)	MAE(Train)	RMS(Test)	MAE(Test)	Parameters	Time(min)
Model-1	1.35	0.84	3.33	1.90	≈15M	4.27
Model-2	1.24	0.61	1.88	1.09	≈37M	9.83

Model-1

The Model-1 with just 5 blocks (downsampling and upsampling) having only 15M parameters was able to achieve a reasonably good result. The model reached an RMSE and MAE value of 1.35 & 0.84 respectively for training images and 3.33 & 1.90 respectively for test images (Table 5.1). Figure 5.3 shows a few test image predicted density maps, its corresponding ground-truth density map, and the animal counts for Model-1.

Model-2

The Model-2 with efficientnet as a feature extractor having 37M parameters outperformed the Model-1 with an RMSE and MAE of 1.24 and 0.61 respectively on training images and 1.88 and 1.09 respectively on test images (Table 5.1). Figure 5.3 shows a few output prediction and corresponding ground-truth for test images.

Table 5.1 show the comparison between Model-1 and Model-2. The average RMSE and MAE for training and test dataset and training time per epoch are given in the table.

5.3 Discussion

To verify the effectiveness of our proposed network architecture, we compare our solution with the Kaggle competition winning model (named *Model-K* from now on) [31] and Count-ception [38], a redundant counting approach based on Inception modules and fully convolutional network. In this section, we consider only our best-performing model, which is Model-2. Table 5.2 shows a comparison of RMSE and MAE for actual and predicted count between the Model-2, Model-K, and Count-ception.

Table 5.2: Comparison between Model-2, Model-K, and Count-ception

Model	Feature Extractor	RMSE	MAE	Parameters
Model-2	Eff.Net-B5	1.88	1.09	≈37M
Model-K	VGG	2.17	1.43	≈48M
Count-ception	*No*	5.57	3.54	≈14M

5.3.1 Comparison with Model-K

The Kaggle winning model (Model-K) [31] architecture is a regression model with VGG16 without top as a feature extractor. The output layer was flattened and given to 2 FC layers with linear output. Model-K was initialized with pre-trained Imagenet weights and then trained using our training dataset. The model was trained using an Stochastic Gradient Descent (SGD) optimizer and an Mean Square Error (MSE) loss function. The trained model was tested with a test dataset and the results are tabulated in Table 5.2.

The Model-K with 48M parameter was able to reach an RMSE and MAE of 2.17 and 1.43 respectively, but our proposed Model-2 with efficientnet feature extractor having 37M parameters gave slightly better results with RMSE and MAE of 1.88 and 1.09 respectively. Our model gave better counting accuracy with lesser model complexity.

5.3.2 Comparison with Count-ception

Count-ception network [38] use Inception modules to build a network targeting at counting object in the image. The whole network is a fully convolutional neural net. In order not to lose pixel information, no pooling layer is used in the architecture. After each convolution, batch normalization and leaky ReLU activation are used to speed up convergence. The model implementation was directly taken from [39]. The model takes an input image and predicts a map. The count from the prediction can be calculated using the below formula;

$$count = \frac{\sum_{x,y} F(I)}{r^2} \tag{5.3}$$

where F(I) is predicted map and r is receptive field size (here, 32) The model was trained and tested with our dataset. For test images the model gave an RMSE and MAE value of 5.85 and 3.81 respectively (Table 5.2). The model had better counting accuracy for images with less overlap, but the accuracy largely dropped when the overlap was high and the sea lions' lay close to the image boundary. In our proposed

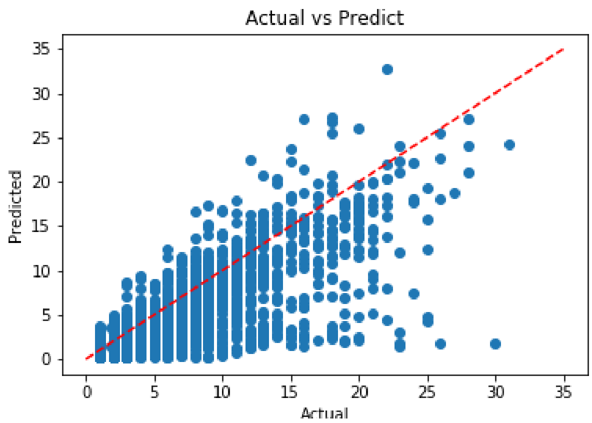

(a) Model-1

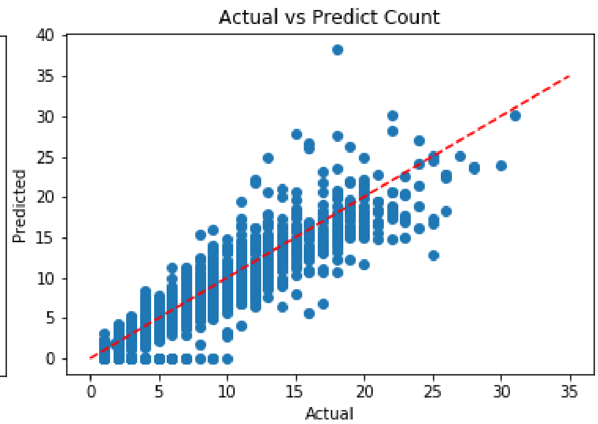

(b) Model-2

Figure 5.2: Actual vs Predicted scatter plot

Gaussian density approach, it treats the object lying close to the boundary as a fraction but Count-ception fails to do it resulting in a decrease in count accuracy.

5.3.3 Visualization

Actual vs Predict Count

To visualize the accuracy of predicted count of proposed Model-2 for test images, we plot an actual vs prediction count scatter plot for both models, as shown in Figure 5.2. The diagonal red line represents the zero error, closer the points to the line better the prediction. The plots show that Model-2 with efficientnet feature extractor has a better prediction result compared to Model-1.

Model Outputs

Figure 5.3 and Figure 5.4 show a few test images together with their actual and predicted density maps and the animal count, for Model-1 and Model-2 respectively. The Figure 5.3,5.4 (images [a-d]) shows few example predcition where the difference between the actual and predicted count is small. Both the models are not heavily affected by different illumination, occlusion, and overlapping. The models were able to perform well despite the challenging environmental conditions like under-water and complex background. Figure 5.3, 5.4 (image [e-f]) show examples of a noticeable difference between the true count and predicted count. The major contribution for the error was from juveniles and pups in the images, this is mainly because;

- Juveniles and pups are inherently difficult to be detected because of their smaller size compared to other sea lion types. The pups look like rocks in the background 5.5(a).

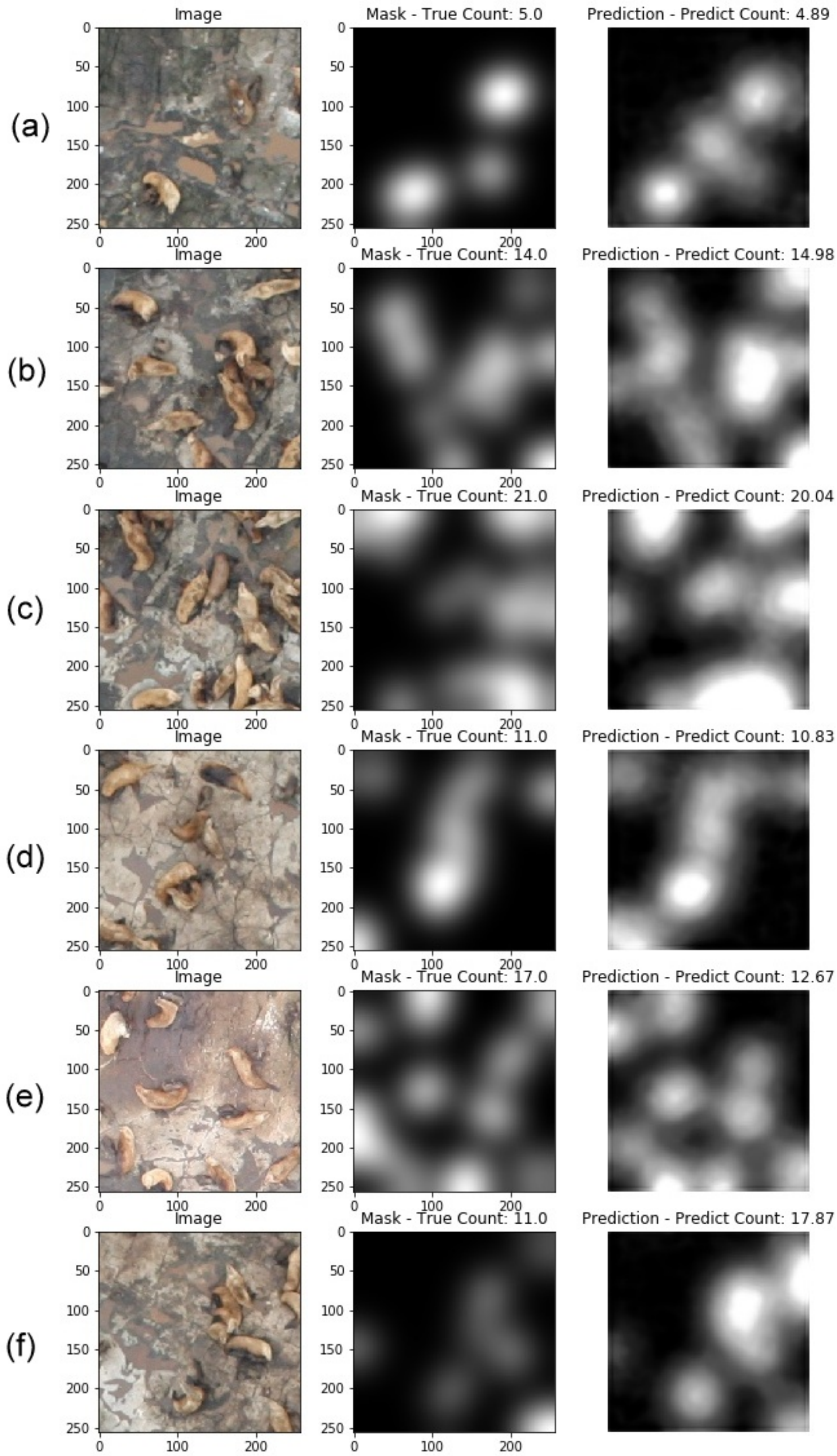

Figure 5.3: Actual vs Predicted density maps for Model-1 and corresponding animal count for test images. From left to right: Input Image, Ground-Truth Density Map, and Predicted Density Map

(a)
(b)
(c)
(d)
(e)
(f)

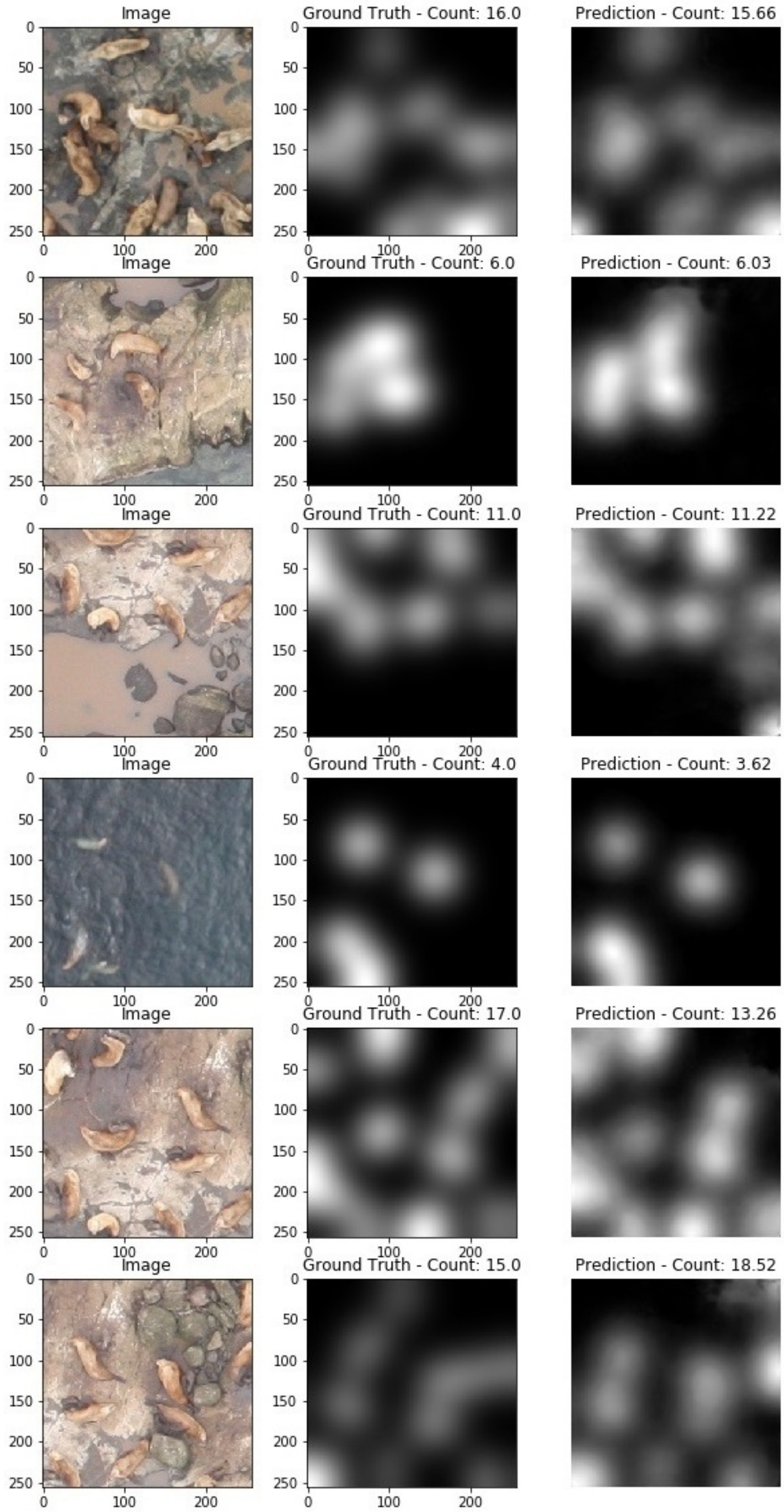

Figure 5.4: Actual vs Predicted density maps for Model-2 and corresponding animal count for test images. From left to right: Input Image, Ground-Truth Density Map, and Predicted Density Map

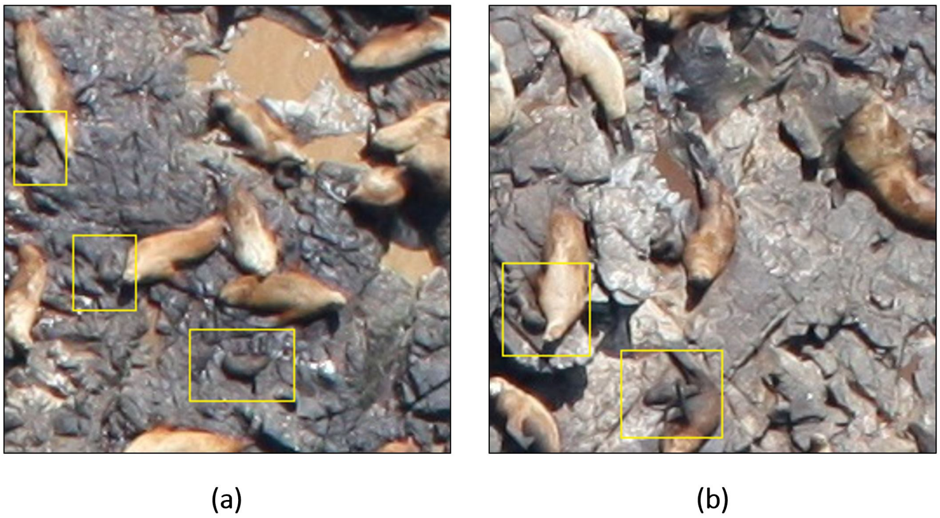

Figure 5.5: Test Image showing the sea lions; (a) Pups looks similar to rocks, (b) Pups lying very close to female sea lion

- The pups usually tend to be closer to female sea lions (possibly their mothers), appearing as part of female sea lions, a fact that makes them hard to be detected, due to occlusion 5.5(b).

5.4 Summary

In this chapter, we carry out the performance evaluation of our proposed models. First, we discuss the training results of our models. Later, we define performance metrics and evaluate & compare the models based on defined performance metrics. To know where we stand, we also compare our results with 2 other models (Kaggle winning model and Count-ception). Finally, we visualize the model outputs and discuss the result.

Chapter 6

Conclusions

Multi-object counting in crowded images is an extremely time-consuming task in real-world application. In a lot of situations, we do not need to detect each object, which means we could avoid the hard problem of detecting individual object instances. Considering this, in this thesis work, we present a solution for sea lion counting from aerial images using deep learning and density map. A semantic segmentation algorithm, *UNet* has been employed for counting task. We utilize the advantages of the Gaussian density map for counting. The tedious pixel-level annotation required for semantic segmentation algorithm is replaced with dot annotation largely reducing annotation overhead.

The results showed that by using *EfficientNet* as a feature extractor architecture, an RMSE of 1.88 was achieved, regardless of the complex background, the different illumination conditions, and the heavy overlapping and occlusion. The proposed solution had a good count prediction with lesser training parameters and minimum annotation. The main error in counting accuracy occurs due to animals' occlusion and small animals (especially, pups) that look like beach rocks. The proposed solution could be extended for counting other wild animals and endangered species as this work provides general implementation rather than specific hand-crafted techniques.

6.1 Future Works

During the course of this thesis work we faced few challenges which could not be addressed fully. Also, there are few ideas which couldn't be implemented due to time limitations and we leave them as possible future improvements.

Ellipsoid Gaussian Density

For this work, we use a circular Gaussian density map as ground-truth (6.1a) even though the density map approach can handle occlusion problems, but when animals are heavily occluded the density map of one animals overlap with other reducing the ability of the model to learn. So having an ellipsoid density map (6.1b) would eliminate the density map pixel overlapping issue. But there rise one more challenge to find the right orientation (i.e. covariance matrix), which could be done by adding one more model to find the alignment of the sea lion.

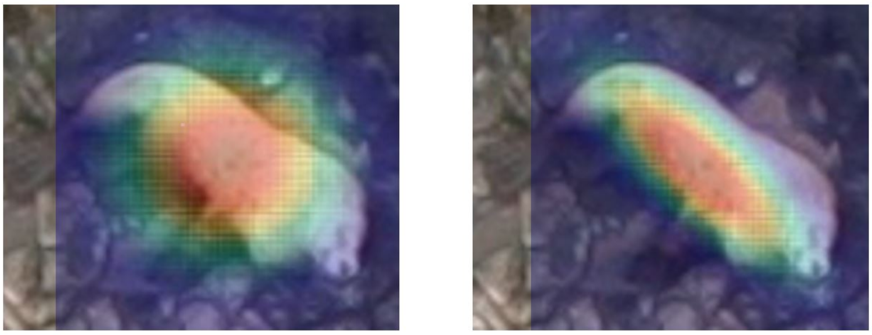

(a) (b)

Figure 6.1: Circular and Ellipsoid Gaussian Density Map super imposed on Adult-male sea lion

Synthetic Dataset

Another approach to increase the prediction accuracy would be with the help of a synthetic dataset. Synthetic data is a dataset that is artificially manufactured rather than generated by real-world events. So by training the model with additional synthetic data might help to improve the detection accuracy.

Class-wise Counting

Presently, we just concentrate on estimating the animal density from the image. In the future, we could also focus on class-wise sea lion counting i.e. we estimate the density map and classify each density to 5 different sea lion classes (Adult male, Sub-adult male, Adult female, Juveniles and Pups) and get class-wise animal count.

Bibliography

[1] “Simple cnn classifier model.” [Online]. Available: https://developers.google.com/machine-learning/practica/image-classification/images/cnn_architecture.svg

[2] “Activation function.” [Online]. Available: https://miro.medium.com/max/1200/1*ZafDv3VUm60Eh10OeJu1vw.png

[3] “Alexnet block diagram.” [Online]. Available: https://missinglink.ai/wp-content/uploads/2019/08/AlexNet-2012.png

[4] “Object detection image.” [Online]. Available: https://www.arunponnusamy.com/images/yolo-object-detection-opencv-python/yolo-object-detection.jpg

[5] “Object detection block diagram.” [Online]. Available: https://miro.medium.com/max/1400/1*NTVoRZYBWbwRxNidyLCxPw.png

[6] R. B. Girshick, J. Donahue, T. Darrell, and J. Malik, “Rich feature hierarchies for accurate object detection and semantic segmentation,” *CoRR*, vol. abs/1311.2524, 2013. [Online]. Available: http://arxiv.org/abs/1311.2524

[7] “Image segmentation.” [Online]. Available: https://miro.medium.com/max/2436/0*QeOs5RvXlkbDkLOy.png

[8] “Image annotation.” [Online]. Available: https://miro.medium.com/max/1400/1*-mnmd7hI1mEAoQBsrRMpLA.jpeg

[9] “Deep learning summary.” [Online]. Available: https://glassboxmedicine.files.wordpress.com/2020/01/coco-task-examples-1.png?w=616

[10] M. Tan and Q. V. Le, “Efficientnet: Rethinking model scaling for convolutional neural networks,” *CoRR*, vol. abs/1905.11946, 2019. [Online]. Available: http://arxiv.org/abs/1905.11946

[11] Y. M. Bar-On, R. Phillips, and R. Milo, “The biomass distribution on Earth,” *Proceedings of the National Academy of Sciences*, vol. 115, no. 25, pp. 6506–6511, jun 2018. [Online]. Available: https://www.pnas.org/content/115/25/6506

[12] S. Diaz, J. Settele, E. Brondizio, H. T. Ngo, M. Gueze, J. Agard, A. Arneth, P. Balvanera, K. Brauman, S. Butchart, K. Chan, L. Garibaldi, K. Ichii, J. Liu, S. M. Subramanian, G. Midgley, P. Miloslavich, Z. Molnar, D. Obura, A. Pfaff, S. Polasky, A. Purvis, J. Razzaque, B. Reyers, R. R. Chowdhury, Y.-J. Shin, I. Visseren-Hamakers, K. Willis, and C. Zayas, "Summary for policymakers of the global assessment report on biodiversity and ecosystem services," Tech. Rep. May 2019, 2019. [Online]. Available: https://www.ipbes.net/news/ipbes/ipbes-global-assessment-summary-policymakers-pdf

[13] J. Kamminga, E. Ayele, N. Meratnia, and P. Havinga, "Poaching detection technologies-A survey," *Sensors (Switzerland)*, vol. 18, no. 5, p. 1474, 2018.

[14] U.S. Fish and Wildlife Service, "Endangered species act," 1973, https://www.fisheries.noaa.gov/topic/laws-policies#endangered-species-act.

[15] N. F. A. F. S. Cente, "Noaa fisheries steller sea lion survey reports." [Online]. Available: https://www.fisheries.noaa.gov/alaska/marine-mammal-protection/steller-sea-lion-survey-reports

[16] N. F. A. F. S. Center, "Noaa fisheries steller sea lion population count." [Online]. Available: https://www.kaggle.com/c/noaa-fisheries-steller-sea-lion-population-count/overview

[17] J. Schmidhuber, "Deep learning in neural networks: An overview," *Neural Networks*, vol. 61, p. 85–117, Jan 2015. [Online]. Available: http://dx.doi.org/10.1016/j.neunet.2014.09.003

[18] Y. Lecun, Y. Bengio, and G. Hinton, "Deep learning," *Nature*, vol. 521, no. 7553, pp. 436–444, 2015.

[19] A. Kamilaris and F. X. Prenafeta-Boldu, "Deep learning in agriculture: A survey," *CoRR*, vol. abs/1807.11809, 2018. [Online]. Available: http://arxiv.org/abs/1807.11809

[20] J. Walsh, N. O' Mahony, S. Campbell, A. Carvalho, L. Krpalkova, G. Velasco-Hernandez, S. Harapanahalli, and D. Riordan, "Deep learning vs. traditional computer vision," 04 2019.

[21] S. Ren, K. He, R. Girshick, and J. Sun, "Faster r-cnn: Towards real-time object detection with region proposal networks," *IEEE Transactions on Pattern Analysis and Machine Intelligence*, vol. 39, no. 6, pp. 1137–1149, 2017.

[22] J. Dai, Y. Li, K. He, and J. Sun, "R-fcn: Object detection via region-based fully convolutional networks," in *Advances in Neural Information Processing Systems 29*, D. D. Lee, M. Sugiyama, U. V. Luxburg, I. Guyon, and R. Garnett, Eds. Curran Associates, Inc., 2016, pp. 379–387. [Online]. Available: http://papers.nips.cc/paper/6465-r-fcn-object-detection-via-region-based-fully-convolutional-networks.pdf

[23] T. Lin, P. Dollár, R. B. Girshick, K. He, B. Hariharan, and S. J. Belongie, "Feature pyramid networks for object detection," *CoRR*, vol. abs/1612.03144, 2016. [Online]. Available: http://arxiv.org/abs/1612.03144

[24] J. Redmon and A. Farhadi, "Yolo9000: Better, faster, stronger," in *2017 IEEE Conference on Computer Vision and Pattern Recognition (CVPR)*, 2017, pp. 6517–6525.

[25] W. Liu, D. Anguelov, D. Erhan, C. Szegedy, and S. Reed, "Ssd: Single shot multibox detector."

[26] T. Lin, P. Goyal, R. Girshick, K. He, and P. Dollár, "Focal loss for dense object detection," *IEEE Transactions on Pattern Analysis and Machine Intelligence*, vol. 42, no. 2, pp. 318–327, 2020.

[27] K.-J. Y. Young-Chul Yoon, "Animal detection in huge air-view images using cnn-based sliding window," *International Workshop on Frontiers of Computer Vision (IWFCV)*, 2018. [Online]. Available: http://hdl.handle.net/10203/244618

[28] J. Liu, C. Gao, D. Meng, and A. Hauptmann, "Decidenet: Counting varying density crowds through attention guided detection and density estimation," 06 2018, pp. 5197–5206.

[29] P. Chattopadhyay, R. Vedantam, R. R. Selvaraju, D. Batra, and D. Parikh, "Counting everyday objects in everyday scenes," in *2017 IEEE Conference on Computer Vision and Pattern Recognition (CVPR)*, 2017, pp. 4428–4437.

[30] M. Rahnemoonfar and C. Sheppard, "Deep count: Fruit counting based on deep simulated learning," *Sensors (Basel, Switzerland)*, vol. 17, 04 2017.

[31] kaggle, "Use keras to count sea lions, kaggle," 2017. [Online]. Available: https://www.kaggle.com/c/noaa-fisheries-steller-sea-lion-population-count/discussion/35408

[32] V. Lempitsky and A. Zisserman, "Learning to count objects in images," in *Advances in Neural Information Processing Systems 23*, J. D. Lafferty, C. K. I. Williams, J. Shawe-Taylor, R. S. Zemel, and A. Culotta,

Eds. Curran Associates, Inc., 2010, pp. 1324–1332. [Online]. Available: http://papers.nips.cc/paper/4043-learning-to-count-objects-in-images.pdf

[33] M. Rahnemoonfar, D. Dobbs, M. Yari, and M. Starek, "Discountnet: Discriminating and counting network for real-time counting and localization of sparse objects in high-resolution uav imagery," *Remote Sensing*, vol. 11, 05 2019.

[34] D. Oñoro and R. López-Sastre, "Towards perspective-free object counting with deep learning," vol. 9911, 10 2016.

[35] M. Tian, G. Hao, H. Chen, Q. Wang, C. Long, and Y. Ma, "Automated pig counting using deep learning," *Computers and Electronics in Agriculture*, vol. 163, p. 104840, 08 2019.

[36] O. Ronneberger, P. Fischer, and T. Brox, "U-net: Convolutional networks for biomedical image segmentation," *CoRR*, vol. abs/1505.04597, 2015. [Online]. Available: http://arxiv.org/abs/1505.04597

[37] P. Yakubovskiy, "Segmentation models," https://github.com/qubvel/segmentation_models, 2019.

[38] J. P. Cohen, H. Z. Lo, and Y. Bengio, "Count-ception: Counting by fully convolutional redundant counting," *CoRR*, vol. abs/1703.08710, 2017. [Online]. Available: http://arxiv.org/abs/1703.08710

[39] S. Banerjee, "Counting sea lions with deep neural networks, count-ception," https://github.com/sbanerj2/count-sea-lion.